

Synthesis of indazole-benzothiadiazole push-pull molecules as solid-state fluorescent compounds

Margot Boujut, Jean-Elie Zheng, Xavier Franck, and Thibault Gallavardin*

Univ Rouen Normandie, INSA Rouen Normandie, CNRS, Normandie Univ, COBRA UMR 6014, INC3M FR 3038, F-76000 Rouen, France

Email: thibault.gallavardin@univ-rouen.fr

Dedicated to Professor Samir Z. Zard, a great scientist and inspiring mentor

Received mm-dd-yyyy

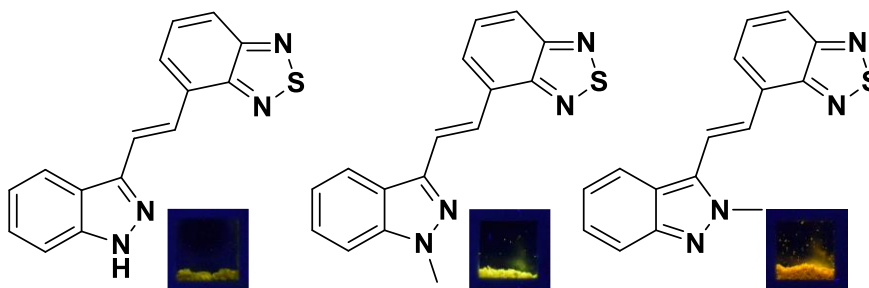
Accepted Manuscript mm-dd-yyyy

Published on line mm-dd-yyyy

Dates to be inserted by editorial office

Abstract

New push-pull fluorophores have been synthesized featuring benzothiadiazole as electron withdrawing group and indazole as electron donating group. This latter group is still scarce in dye chemistry, one of its particularities is that it has labile proton which allows an equilibrium between two tautomeric forms. By performing the methylation of one or the other nitrogen atom each of these forms can be compared independently. Moreover, one of the blocked tautomers leads to an impressive enhancement of the fluorescence in solid state with fluorescent quantum yield increasing from 0.01 to 0.37.



Keywords: Indazole, benzothiadiazole, fluorescence, solid state emission

Introduction

The Indazole scaffold has gained increasing prominence in medicinal chemistry, particularly for the development of tyrosine kinase inhibitors.^{1–3} This prominence arises from the presence of two adjacent nitrogen atoms on the aromatic moiety, enabling strong hydrogen bond formation within the hydrophobic pockets of receptors. However, the utilization of chromophores based on this structure remains scarce.^{4–6} This is due to the challenge of predicting their fluorescence properties, as they may or may not exhibit efficient intersystem crossing resulting in low fluorescence quantum yields.⁷ Additionally, nitrogen-containing fluorophores can be strongly influenced by hydrogen bonds and pH. We recently synthesized merocyanine mitochondria markers using indazole as electron-donating group, demonstrating added-value compared to the more commonly employed indole nucleus.⁸

Indazole 1 is a heteroaromatic molecule that exhibits a tautomeric equilibrium between a so called “aromatic” form and a “quinoid” form (

Figure 1). This equilibrium had been extensively studied by Catalan in non-functionalized indazole, revealing that the aromatic form is more stable than the quinoid at both ground and excited states.^{9,10}

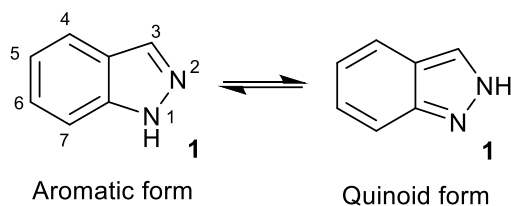


Figure 1. Tautomeric equilibrium in non-functionalized indazole **1**.

This characteristic becomes even more pronounced when indazole is incorporated into extended π -conjugated systems. In such cases, this duality can significantly impact the electrons delocalization throughout the entire of push-pull chromophore framework. To investigate this phenomenon and study the properties of both tautomers independently, we blocked each tautomer through alkylation. To achieve this, a push-pull molecule **2** was synthesized by connecting the position 3 of indazole with the electron-poor benzothiadiazole moiety, using an alkene spacer (Figure 2). Benzothiadiazole was chosen because it is reported for its ability to promote strong fluorescence in dipolar compounds.^{11–13} The optical properties of this molecule were then compared with those of the corresponding blocked N-methylated tautomers **3** (N-1) and **4** (N-2) in solution and in condensed phase.

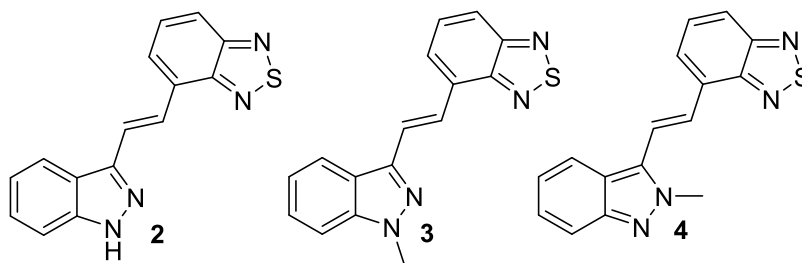


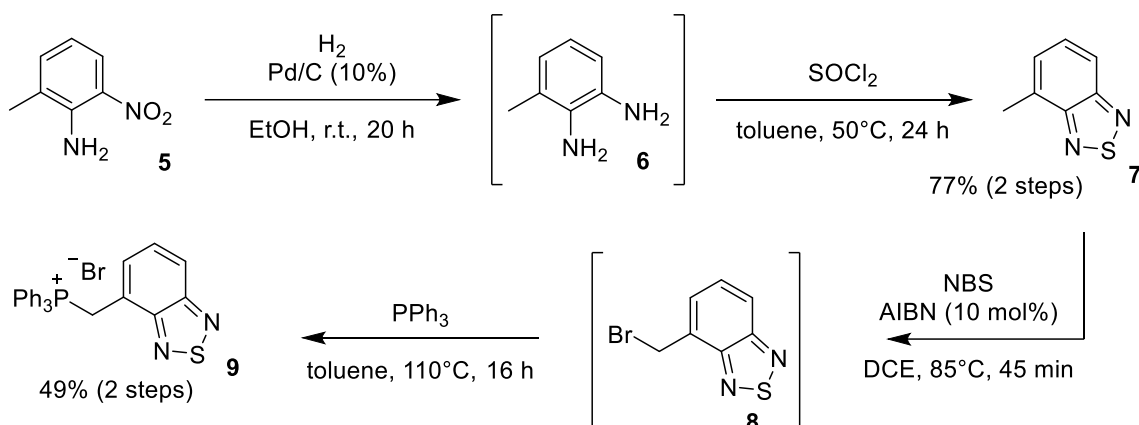
Figure 2. Structures of Indazole benzothiadiazole push-pull molecules.

Results and Discussion

Synthesis

Several syntheses of indazole compounds bearing an alkene moiety in position 3 have been previously reported. These syntheses rely either on the formation of the five atoms ring of indazole through a cyclisation reaction,^{14,15} the building of the alkene bond by Knoevenagel reaction,¹⁶ Heck palladium cross-coupling,^{17,18} C-H activation,^{19,20} or a Wittig reaction.²¹ Here the latter option was chosen, starting from the benzothiadiazole (BTD) phosphonium salt **9** and protected indazole aldehyde **12**. The phosphonium salt **9** was prepared from nitroaniline **5** which was reduced to the diamino compound **6** by Pd/C catalyzed hydrogenation. **6** was then reacted, without purification, with SOCl₂ to provide the 4-methylated benzothiadiazole **7** (77% over two steps)

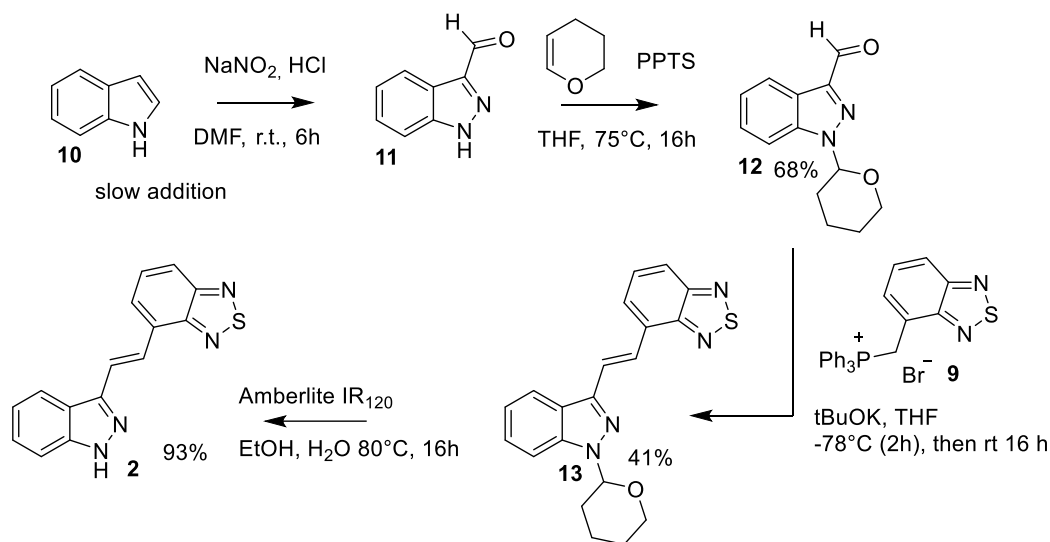
(Scheme 1). This latter was brominated by radical reaction with NBS initiated by AIBN. Purification of **8** proved to be difficult due to the formation of a mixture of mono- and di-brominated compounds. To address this issue, triphenylphosphine was directly added to this mixture, resulting in the formation of the phosphonium salt **9** which was easily purified by precipitation (49% over two steps).



Scheme 1. Synthesis of benzothiadiazole phosphonium salt.

On the other hand, the THP protected 3-indazolecarbaldehyde **12** was prepared in two steps (

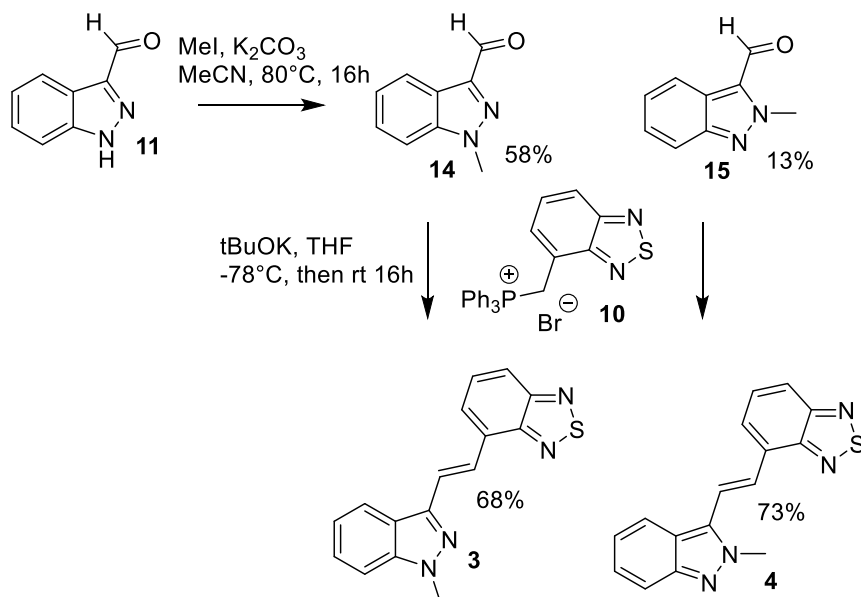
Scheme 2), using our previously described nitrosation of indoles protocol,²² by slow addition of indole in a solution of NaNO₂ in HCl. During this reaction, two key factors play a significant part to the success of this reaction: the slow addition of indole to the nitrosonium solution reduces the local concentration of indole to avoid its dimerization, and the pH has to be kept neutral by using HCl as the limiting reagent to prevent the formation of diazonium salts. Then the so-obtained aldehyde **11** was protected by a THP group (tetrahydropyran) by reaction with DHP (dihydropyran) in presence of PPTS (pyridium *p*-toluenesulfonate) under thermodynamic conditions.²³ This reaction selectively led to the functionalization of the nitrogen atom in position 1, giving the 1-THP protected 3-indazolecarbaldehyde (**12**) in 68% yield over the two steps. Then the Wittig reaction was conducted by deprotonation of the phosphonium salt **9** by tBuOK at low temperature (Scheme 2). The reaction was then completed at room temperature to give the alkene **13** as a single (*E*)-isomer and with 41% yield. Finally, a delicate deprotection reaction was carried out in soft acidic medium by Amberlite® IR120.²⁴ The desired free indazole **2** was then recovered in 93% yield after a simple filtration.



Scheme 2. Synthesis of non-methylated compound **2**.

The synthesis of methylated derivatives **3** and **4** followed a similar sequence (

Scheme 3); first a non-selective methylation of nitrogen atoms of **11** was carried out to produce both *N*-1 and *N*-2 separable regioisomers **14** (58%) and **15** (13%), respectively. These regioisomers were identified by ¹H NMR using previously published data.²⁵ Then a Wittig reaction in the same conditions as above afforded *N*-1 **3** and *N*-2 **4** locked tautomers with 68% and 73% yield, respectively. The regioisomers **3** and **4** can be discriminated by NOESY NMR experiments (see supporting information) thanks to a correlation in molecule **4** between the *N*-2 methyl group (δ : 4.31 ppm) and one of the olefinic hydrogens (δ : 8.52 ppm).



Scheme 3. Synthesis of methylated compounds **3** and **4**.

Optical properties

Absorption and emission of **2**, **3** and **4** were recorded in dichloromethane (Figure 3). Methylation produced a noticeable effect both in absorption and emission. Starting from 400 nm for non-methylated **2**, the methylation in position 1 of **3** induced a 10 nm red shift in absorption originating from the inductive effect of the methyl group, making indazole a stronger electron donating group. With compound **4** (*N*-2 methylated), the absorption is even more red shifted i.e. 30 nm compared to **2**, as the methylation in this position locks indazole in “quinoid form”. Being less aromatic, this form promotes electron delocalization increasing the push-pull character of this molecule.²⁶ In emission, the trend was exactly the same, with a maximum at 530 nm for **2**, 551 nm for **3** and 584 nm for **4**. High fluorescence quantum yields ranging from 0.92, 0.96 and 0.77 for **2**, **3** and **4** respectively were measured in dichloromethane, showing once more that **2** and **3** have close electronic structures. Compounds **2** and **3** featured long excited state lifetimes ($\tau_f \approx 10$ ns) demonstrating that non-radiative deexcitations are very small in this system, in the other hand, the lifetime of **4** was shorter ($\tau_f \approx 8$ ns). While both the lifetime and fluorescence quantum yield of **4** are reduced, the radiative constant of **4** remains similar to those of **2** and **3** ($k_r \approx 9-10$ s⁻¹) showing that fluorescence quenching originates from the appearance of a new non-radiative pathway in compound **4** (Table 1).

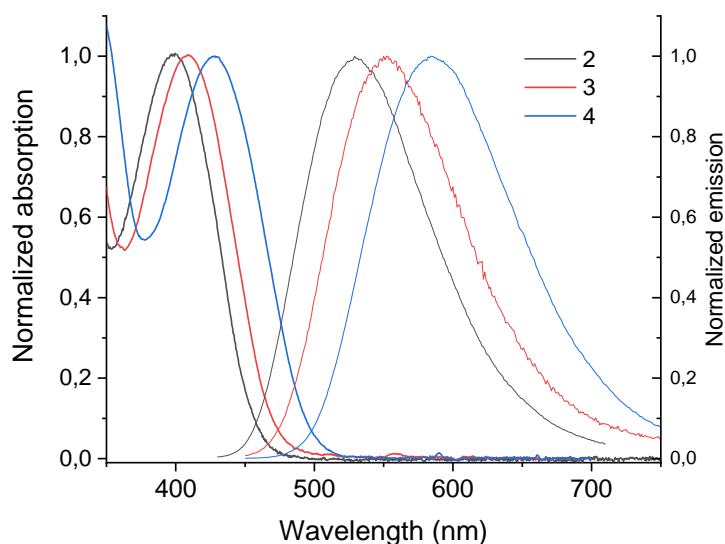


Figure 3. Absorption and emission in dichloromethane.

Table 1. Optical properties of compounds 2, 3 and 4 solubilized in dichloromethane.

	λ_{abs} (nm)	λ_{em} (nm)	Stokes shift (cm ⁻¹)	ϵ (L.mol ⁻¹ cm ⁻¹)	ϕ_f^a	$\langle\tau_f\rangle$ (ns)	k_r (s ⁻¹)
2	400	530	6220	10200	0.92	10.1	$9.0 \cdot 10^7$ s ⁻¹
3	410	551	6365	10300	0.96	10.0	$9.9 \cdot 10^7$ s ⁻¹
4	430	584	6240	13900	0.77	8.4 ^b	$9.2 \cdot 10^7$ s ⁻¹

^a measured using coumarin 153 as standard (0.54 in EtOH), ^b biexponential.

Because of their push-pull structure, these molecules feature solvatochromism (

Figure 4) from around 510 nm in toluene to 610-650 nm in methanol. However, molecule **2** shows superimposed emission spectra in tetrahydrofuran, dioxane, chloroform and dichloromethane at 525 nm while they are well separated for **3**. This highlights the presence of donating hydrogen bonds between the proton of **2** and the oxygen atoms of tetrahydrofuran and dioxane which makes indazole more electron

donating, leading to a small red shift in these two solvents and superimposition with dichloromethane/chloroform emission spectra. The spectra of **4** are red shifted (30 nm) by comparison with those of **3** but their order and shapes are very similar.

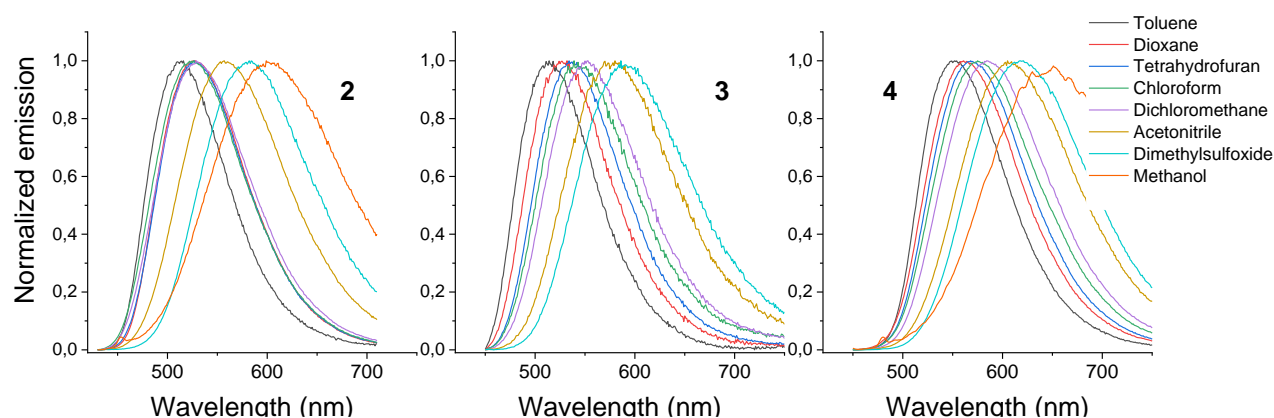


Figure 4. Solvatochromism of molecules **2**, **3** and **4**.

To better describe the solvatochromism, the $E_T(30)$ scale, an empirical solvent polarity scale, can be used.²⁷ Emission energies of the compounds are plotted against $E_T(30)$ values and should give linear regression if only solvent polarity affects emission wavelengths (Figure 5). In the case of molecule **2**, the fitting of the linear regression is dissatisfactory as four points are aligned at an emission energy of 19000 cm^{-1} . Indeed, in dioxane ($E_T(30)=36$) and in THF ($E_T(30) = 37,4$) the energy is lowered by hydrogen bond formation between the free lone pairs of these solvents and the labile proton of indazole **2**. This effect is even more pronounced in dimethylsulfoxide ($E_T(30) = 45,1$), making difficult the determination of a reliable slope. On the other hand, in methanol ($E_T(30) = 55,4$), the point is above the curves for all compounds which shows that indazole is an hydrogen bond acceptor.

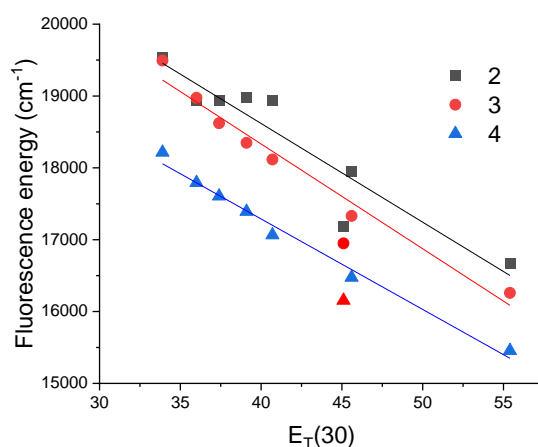


Figure 5. Solvatochromism of compounds **2**, **3** and **4** using $E_T(30)$ solvent polarity scale.

Solid state emission

Methylation can also affect the optical properties of these compounds in solid state as it prevents hydrogen bonding between molecules, which should alter their spatial arrangement. Compounds **2**, **3** and **4** powders are fluorescent upon exposure to UV lamp (Figure 6a).

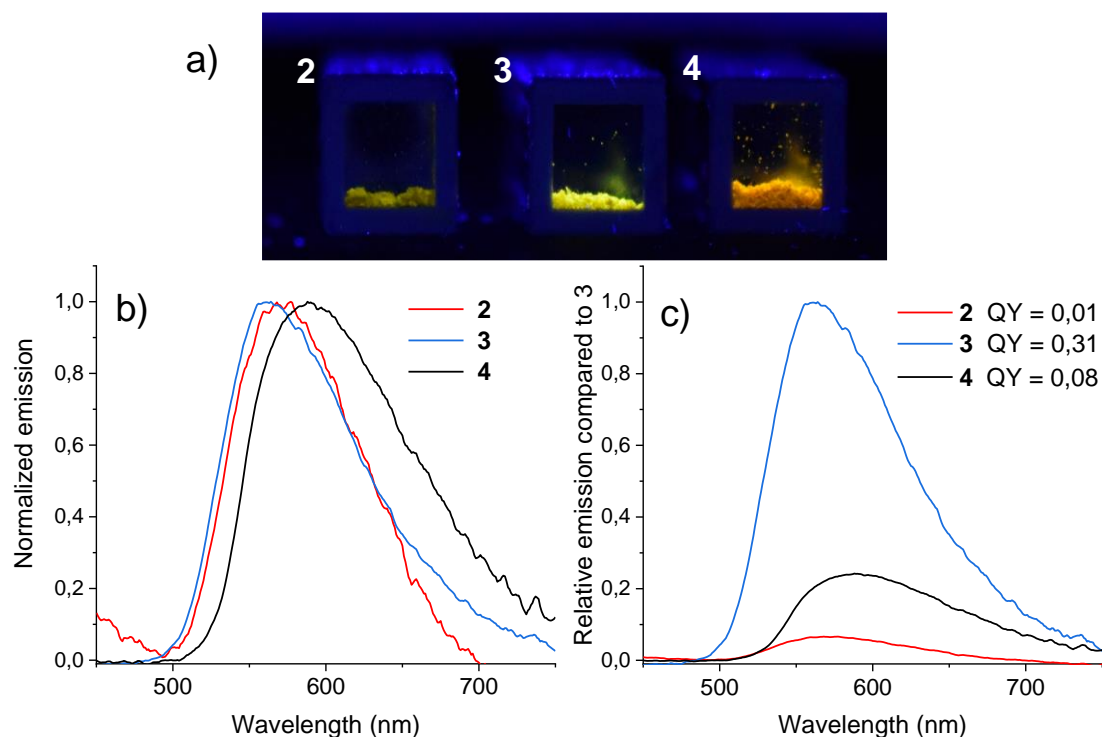


Figure 6. a) Photo of **2**, **3** and **4** (from left to right) under UV light irradiation. Normalized emission in solid state. b) normalization by division by maximum. c) relative normalization by the area under the curves proportional to their relative quantum yields.

The determination of both their spectral shape and their solid-state fluorescent quantum yield was achieved by using an integrating sphere (Figure 6b). Compound **2** turned out to be only slightly fluorescent, with a low quantum yield of 0.01 and an emission peak at 560 nm. The two methylated compounds featured stronger fluorescence with respectively an impressive 0.31 for compound **3** (570 nm) and 0.08 (600 nm) for compound **4**. These emission wavelengths are close to those measured in acetonitrile. Fluorescence quenching in solid-state for molecule **2** might be related to vibrations of the NH bond or to intermolecular bonding which can modify the packing of the molecules. The emission maximum of compounds **2** and **3** were very similar, the inductive effect of the methyl observed in solution is no more present. This suggest that the molecular packing is different for these two molecules which could explain the big difference in fluorescence intensity. Compound **4** exhibits a 30 nm red-shift in comparison to **3**, in line with our in-solution measurements. Surprisingly, this red shift coincides with a lower quantum yield. To visually compare their solid-state emissions, (Figure 6c) presents their relative emissions: **3** is normalized, while **2** and **4** are plotted to ensure that the area under the curve is proportional to their relative quantum yields relative to **3**. This highlights the substantial difference in fluorescence efficiency between the molecules.

Conclusions

Three push-pull molecules were synthesized, each containing an indazole as an electron-donating group and a benzothiadiazole as an electron-withdrawing group. These molecules were prepared using a Wittig reaction to investigate the impact of methylation at nitrogen atoms in positions 1 and 2. As expected, these molecules

exhibited significant fluorescence solvatochromism demonstrating the suitability of indazole as electron donating group. Methylation had a substantial effect on the optical properties of the molecules, resulting in a red shift in both absorption and fluorescence emission. The most pronounced effect was observed in powder state where methylation led to a substantial increase in the fluorescence quantum yield, particularly for molecule **3** which exhibited an impressive quantum yield of 0.31. This makes this molecule very attractive for applications as a fluorescent pigment.

Experimental Section

General. All reagents and solvents were commercial grade and purified prior to use when necessary. THF was distilled from Na under argon immediately before use. Thin layer chromatography (TLC) was performed using aluminum-backed silica gel (225 μm) plates and flash chromatography utilized 230–400 mesh silica gel from Sigma-Aldrich. Products were visualized by UV light, and/or the use of ceric ammonium molybdate. IR spectra were recorded on a Nicolet™ iSTM5 FT-IR Spectrometer and are reported in wavenumbers (cm^{-1}). Liquids and oils were analyzed as neat films on a NaCl plate (transmission), whereas solids were applied to a diamond plate (ATR). Nuclear magnetic resonance spectra (NMR) were acquired on a Bruker Avance III-300 (300 MHz), BBFO probe. Chemical shifts were measured relative to residual solvent peaks as an internal standard set to δ 7.26 and δ 77.1 (CDCl_3) or 2.05 and 29.84, 206.3 ($\text{CO}(\text{CD}_3)_2$), or 2.50 and 39.52 ($\text{SO}(\text{CD}_3)_2$). HRMS FAB data was collected from a LC-HRMS Thermo LQC Bruker trap HCT ultra ETD mass Spectrometer at the COBRA laboratory.

Optical measurement methods. UV-visible absorption spectra were recorded using a Cary 60 (Agilent) spectrophotometer applying a baseline correction in 1 cm path length quartz cuvettes.

Steady state fluorescence spectra were measured with a Fluorolog 3–21 (Horiba, Hamamatsu photomultiplier tube R13456) using diluted samples O.D. < 0.1 in 3.5 mL cuvettes. In solution, fluorescence quantum yields (ϕ_f) were measured following this equation: $\phi_f = \phi_{F_c} \times [F/F_c] \times [(1-10^{-A})/(1-10^{-A_c})] \times [n/n_c]^2$ where “F” is the integrated fluorescence signal of the dye, “F_c” is the integrated fluorescence signal of the reference (coumarin 153 in ethanol, $\phi_{F_c} = 0.54$ described by Rurack);²⁸ A and A_c are the absorbances the dye and the coumarin 153 respectively; n and n_c the refractive index of the solvents: dye (dichloromethane) and reference (ethanol).

Fluorescence lifetimes were measured by TCSPC using an EPL 405 nm LASER diode (5 mW, pulse width 56.3 ps, repetition rate 200 ns, Edinburgh Instrument). The measurement stopped when the maximum number of counts reached 10 000.

Solid state emission was measured in an integrating sphere G8 (General Microtechnology and Photonics) fitted inside a Horiba Fluorolog 3–21. The corrected spectra were measured and the blank signal was subtracted, considering the extinction caused by the sample. Quantum yields were calculated (excitation 420 nm) using the following equation: $\phi_f = (f_p - (I_p/I_s) \times f_s)/(F_i \times (I_s - I_p))$ where f_p and f_s are fluorescence signals (450–750 nm) with and without product respectively F_i is the transmission of a 1% DO filter (Thorlabs) at excitation wavelength and I_p and I_s are lamp signal (400–420 nm) with and without product respectively.

4-(2-(1H-Indazol-3-yl)vinyl)benzo[c][1,2,5]thiadiazole (2). To a solution of 1-(tetrahydro-2H-pyran-2-yl)-1H-indazole (**13**) (28 mg, 0.08 mmol, 1 eq.) in EtOH (final concentration of 0.01 M) and H₂O (2% v/v), the cation exchanger resin Amberlite IR120 (80 mg) was added. The mixture was heated to 80°C under inert atmosphere for 16 hours. The suspension was hot filtered, and the resin washed twice with hot EtOH. The solution was

dried over MgSO₄, concentrated under reduced pressure. (20 mg, yellow powder, 93% yield of isolated product). **¹H NMR (CO(CD₃)₂, 300 MHz)**. δ (ppm) 8.53 (d, 1H, *J* 16.5 Hz), 8.24 (dt, 1H, *J* 8.0, 1.0 Hz), 8.10 (d, 1H, *J* 16.5 Hz), 8.01 – 7.94 (m, 2H), 7.77 (dd, 1H, *J* 8.5, 7.0 Hz), 7.65 (dt, 1H, *J* 8.5, 1.0 Hz), 7.45 (ddd, 1H, *J* 8.0, 7.0, 1.0 Hz), 7.29 (ddd, 1H, *J* 8.0, 7.0, 1.0 Hz). **¹³C NMR (CO(CD₃)₂, 75 MHz)**. δ (ppm) 156.6, 154.1, 143.9, 142.7, 131.7, 131.0, 128.1, 127.3, 127.0, 126.5, 122.2, 122.1, 121.4, 120.9, 111.4. **IR**: ν (cm⁻¹) 3152, 3119, 2914, 1627, 1534, 1462, 1341, 1253, 1094, 728. **HRMS (ESI⁺)**: [**M+H**]⁺ found 279.0716; calculated for [C₁₅H₁₁N₄S]⁺ 279.0704. **mp** decomposition > 205°C.

4-(2-(1-Methyl-1*H*-indazol-3-yl)vinyl)benzo[*c*][1,2,5]thiadiazole (3). At -78°C, *t*BuOK (1.1 eq.) was added to a suspension of aldehyde **15** (40 mg, 0.25 mmol, 1 eq.) and the Wittig salt **10** (134 mg, 0.28 mmol, 1 eq.) in dry THF (2.5 mL). The mixture was left 2 hours at -78°C then brought back to room temperature until completion before being quenched by addition of water and extracted with EtOAc. The crude product was purified by flash chromatography (cyclohexane: EtOAc 95:5). (50 mg, bright yellow powder, 68% yield of isolated product). **¹H NMR (CO(CD₃)₂, 300 MHz)**. δ (ppm) 8.49 (d, 1H, *J* 16.5 Hz), 8.21 (dt, 1H, *J* 8.5, 1.0 Hz), 8.06 (d, 1H, *J* 16.5 Hz), 8.00 – 7.92 (m, 2H), 7.76 (dd, 1H, *J* 8.5, 7.0 Hz), 7.64 (dt, 1H, *J* 8.5, 1.0 Hz), 7.52 – 7.44 (ddd, 1H, *J* 8.0, 7.0, 1.0 Hz), 7.30 (ddd, 1H, *J* 8.0, 7.0, 1.0 Hz), 4.14 (s, 3H). **¹³C NMR (CO(CD₃)₂, 75 MHz)**: δ (ppm) 155.7, 153.1, 141.5, 141.4, 130.8, 130.0, 127.1, 126.3, 125.6, 125.2, 122.1, 121.2, 120.6, 119.9, 109.8, 35.0. **IR**: ν (cm⁻¹) 2926, 1743, 1451, 1247, 1066, 962, 740. **HRMS (ESI⁺)**: [**M+H**]⁺ found 293.0859; calculated for [C₁₆H₁₃N₄S]⁺ 293.0861. **mp** 158-159°C.

4-(2-(2-Methyl-2*H*-indazol-3-yl)vinyl)benzo[*c*][1,2,5]thiadiazole (4). At -78°C, *t*BuOK (1.1 eq.) was added to a suspension of aldehyde **16** (40 mg, 0.25 mmol, 1 eq.) and the Wittig salt **10** (134 mg, 0.28 mmol, 1 eq.) in dry THF (2.5 mL). The mixture was left 2 hours at -78°C then brought back to room temperature until completion before being quenched by addition of water and extracted with EtOAc. The crude product was purified by flash chromatography (cyclohexane: EtOAc 95:5). (53 mg, bright orange powder, 73% yield of isolated product). **¹H NMR (CO(CD₃)₂, 300 MHz)**. δ (ppm) 8.59 (d, 1H, *J* 16.5 Hz), 8.17 (dt, 1H, *J* 8.5, 1.0 Hz), 8.04 (d, 1H, *J* 7.0 Hz), 7.99 (dd, 1H, *J* 8.5, 1.0 Hz), 7.97 (d, 1H, *J* 16.5 Hz), 7.77 (dd, 1H, *J* 8.5, 7.0 Hz), 7.67 (dt, 1H, *J* 8.5, 1.0 Hz), 7.33 (ddd, 1H, *J* 8.5, 7.0, 1.0 Hz), 7.22 (ddd, 1H, *J* 8.5, 7.0, 1.0 Hz), 4.37 (s, 3H). **¹³C NMR (CO(CD₃)₂, 75 MHz)**. δ (ppm) 156.6, 153.9, 149.0, 133.4, 131.3, 130.9, 128.7, 127.2, 126.5, 123.3, 121.5, 121.5, 121.3, 121.0, 118.6, 38.8. **IR** ν (cm⁻¹) 3069, 2926, 2855, 1622, 1462, 1291, 1249, 1050, 954, 747. **HRMS (ESI⁺)**: [**M+H**]⁺ found 293.0870; calculated for [C₁₆H₁₃N₄S]⁺ 293.0861. **mp** 143-145°C.

4-Methylbenzo[*c*][1,2,5]thiadiazole (7). 2-amino-3-nitrotoluene (4.56 g, 30 mmol) was solubilized in EtOH (300 mL) and the solution was purged under a nitrogen flow. After 15 min, palladium on charcoal (10% w/mol) was added, then nitrogen gas was evacuated under vacuum and hydrogen was added (balloon). The reaction was left to proceed under a hydrogen atmosphere at room temperature. The suspension was filtered on a celite pad and the solvent removed under reduced pressure. The crude product was dissolved in toluene (200 mL) and cooled to 0°C. Thionyl chloride (100 mL, 50 eq.) was added over 1 h via a dropping funnel then the reaction was heated to 50°C for 24 h. The excess thionyl chloride was **very carefully** quenched at 0°C by pouring the crude mixture on a solution of aqueous NaOH (1 M). The mixture was diluted with 1 L of water and heated to 140°C and steam distilled until 1 L of solution was collected. This latter fraction was saturated with NaCl and extracted by EtOAc. The crude product was used without any further purification (3.45 g, light yellow oil, 77% yield of isolated product). **¹H NMR (CDCl₃, 300 MHz)**. δ (ppm) 7.83 (dt, 1H, *J* 9.0, 1.0 Hz), 7.49 (dd, 1H, *J* 9.0, 7.0 Hz), 7.37 – 7.31 (dq, 1H, *J* 7.0, 1.0 Hz), 2.75 (t br, 3H, *J* 1.0 Hz). **¹³C NMR (CDCl₃, 75 MHz)**. δ (ppm) 155.6, 155.1, 131.8, 129.7, 128.1, 119.1, 18.0. **IR**: ν (cm⁻¹) 2972, 2920, 1605, 1575, 1485, 1153, 898, 853, 828, 797, 752. **HRMS (ESI⁺)**: [**M+H**]⁺ found 151.03359; calculated for [C₇H₇N₂S]⁺ 151.03299.

(Benzo[c][1,2,5]thiadiazol-4-ylmethyl)triphenylphosphonium bromide (9). To a solution of 4-methylbenzo[c][1,2,5]thiadiazole (1.50 g, 10 mmol) in dry DCE (50 mL), NBS (1.94 g, 1.1 eq.) and AIBN (0.16 g, 0.1 eq.) were successively added. The reaction was heated to 85°C under argon for 1 h. The solution was treated with aq. Na₂S₂O₃ and extracted with DCM. The organic layers were concentrated under reduced pressure. The crude mixture was dissolved in toluene (100 mL) in the presence of PPh₃ (10.5 g, 4 eq.) and the solution was heated to 110°C until completion. The mixture was brought back to room temperature and the resulting precipitate was filtered. The crude solid was washed twice with toluene and dried under reduced pressure to afford **9** which was used without any further purification (2.42 g, light yellow powder, 49% yield of isolated product). ¹H NMR (SO(CD₃)₂, 300 MHz). δ (ppm) 8.02 (dd, 1H, *J* 9.0, 2.5 Hz), 7.89 – 7.79 (m, 3H), 7.78 – 7.59 (m, 13H), 7.50 (dd, 1H, *J* 7.0, 4.0 Hz), 5.64 (d, 2H, *J* 15.4 Hz). ¹³C NMR (SO(CD₃)₂, 75 MHz). δ (ppm) 154.0 (d, *J* 4.0 Hz), 153.8 (d, *J* 2.5 Hz), 135.1 (d, *J* 3.0 Hz), 133.9 (d, *J* 10.0 Hz), 131.7 (d, *J* 7.5 Hz), 130.0 (d, *J* 12.5 Hz), 129.7 (d, *J* 4.5 Hz), 121.6 (d, *J* 4.0 Hz), 121.2 (d, *J* 9.5 Hz), 117.5 (d, *J* 85.5 Hz), 25.24 (d, *J* 50.0 Hz). ³¹P NMR (SO(CD₃)₂, 121 MHz). δ (ppm) 23.2. IR ν (cm⁻¹) 2998, 1677, 1434, 1104, 741, 687, 489. HRMS (ESI⁺): [M]⁺ found 411.1082; calculated for [C₂₅H₂₀N₂PS]⁺ 411.1085. mp 218-221°C.

1H-Indazole-3-carbaldehyde (11). At 0°C, under argon atmosphere, aqueous HCl (2 M, 40 mL, 2.67 eq.) was added to a solution of NaNO₂ (16.6 g, 3 eq.) in water (120 mL) and DMF (130 mL). Then the solution of indole (3.51 g, 30 mmol) in DMF (40 mL) was added dropwise over a 2-hour period with a syringe-pump. At the end of the addition, the mixture was brought back to room temperature and stirred for 16h. A large volume of water was added and the mixture extracted with EtOAc, then the organic layers were further washed with water and brine. The crude product was used without any further purification (4.10 g, white powder, 94 % yield of isolated product). ¹H NMR (CDCl₃, 300 MHz). δ (ppm) 10.29 (s, 1H), 8.31 (dt, 1H, *J* 8.0, 1.0 Hz), 7.59 (dt, 1H, *J* 8.5, 1.0 Hz), 7.46 (ddd, 1H, *J* 8.5, 7.0, 1.0 Hz), 7.34 (ddd, 1H, *J* 8.0, 7.0, 1.0 Hz). ¹³C NMR (SO(CD₃)₂, 75 MHz). δ 187.4, 143.4, 141.1, 127.3, 123.8, 120.7, 120.2, 111.2; IR ν 3254, 3174, 1671, 1458, 1331, 1251, 1092, 792 and 739 cm⁻¹; HRMS (ESI⁻): [M-H]⁻ found: 145.0402; calculated for [C₈H₅N₂O]⁻ 145.0390.

1-(Tetrahydro-2H-pyran-2-yl)indazole-3-carbaldehyde (12). 3,4-Dihydro-2H-pyran (DHP, 5.5 mL, 6 eq.) and pyridium *p*-toluenesulfonate (PPTS; 302 mg, 0.2 eq.) were successively added to a solution of 1H-indazole-3-carbaldehyde **11** (1.46 g, 10 mmol) in dry THF (100 mL). The reaction was heated to 75°C until completion. A large volume of water was added then the mixture was extracted with EtOAc. The crude product was purified by flash chromatography (cyclohexane 100%) (1.56 g, white powder, 68% yield of isolated product). ¹H NMR (CDCl₃, 300 MHz). δ (ppm) 10.26 (s, 1H), 8.31 (dt, 1H, *J* 8.0, 1.0 Hz), 7.68 (dt, 1H, *J* 8.5, 1.0 Hz), 7.48 (ddd, 1H, *J* 8.5, 7.0, 1.0 Hz), 7.37 (ddd, 1H, *J* 8.0, 7.0, 1.0 Hz), 5.85 (dd, 1H, *J* 8.5, 2.5 Hz), 4.06 – 3.99 (m, 1H), 3.84 – 3.73 (m, 1H), 2.67 – 2.52 (m, 1H), 2.23 – 2.07 (m, 2H), 1.86 – 1.69 (m, 3H). ¹³C NMR (CDCl₃, 75 MHz). δ (ppm) 187.4, 143.5, 140.9, 127.7, 124.4, 122.5, 122.3, 110.8, 86.2, 67.5, 29.3, 25.1, 22.2. IR: ν (cm⁻¹) 2942, 2870, 2798, 1689, 1473, 1318, 1225, 1077, 913, 787, 747. HRMS (ESI⁺): [M+H]⁺ found 231.1130; calculated for [C₁₃H₁₅N₂O₂]⁺ 231.1134. mp 70-73°C.

4-(2-(1-(Tetrahydro-2H-pyran-2-yl)indazol-3-yl)vinyl)benzo[c][1,2,5]thiadiazole (13). At -78°C, *t*BuOK (31 mg, 0.28 mmol, 1.1 eq.) was added to a suspension of aldehyde **12** (58 mg, 0.25 mmol, 1 eq.) and the phosphonium salt **9** (134 mg, 0.28 mmol, 1 eq.) in dry THF (2.5 mL). The mixture was left 2 hours at -78°C then brought back to room temperature until completion. The crude mixture was neutralized by addition of water and extracted with EtOAc. The crude product was purified by flash chromatography (cyclohexane: EtOAc 95:5) to give 37 mg of **13** as a yellow powder (41% yield of isolated product). ¹H NMR (CDCl₃, 300 MHz). δ (ppm) 8.36 (d, 1H, *J* 16.5 Hz), 8.15 (d, 1H, *J* 8.0 Hz), 8.05 (d, 1H, *J* 16.5 Hz), 7.92 (dd, 1H, *J* 8.5, 1.0 Hz), 7.74 (d, 1H, *J* 7.0 Hz), 7.66 – 7.58 (m, 2H), 7.45 (ddd, 1H, *J* 8.5, 7.0, 1.0 Hz), 7.30 (ddd, 1H, *J* 8.0, 7.0, 1.0 Hz), 5.77 (dd, 1H, *J* 9.5, 2.5 Hz), 4.16 – 4.03 (m, 1H), 3.78 (dt, 1H, *J* 11.0, 2.5 Hz), 2.75 – 2.56 (m, 1H), 2.27 – 2.02 (m, 2H), 1.89 – 1.65

(m, 3H). ^{13}C NMR (CDCl_3 , 75 MHz). δ (ppm) 155.8, 153.5, 143.3, 141.0, 131.0, 129.8, 126.9, 126.8, 126.7, 125.4, 123.2, 122.0, 121.3, 120.4, 110.5, 85.7, 67.8, 29.7, 25.3, 22.8. IR. ν (cm^{-1}) 3076, 2922, 2856, 1689, 1474, 1318, 1224, 1035, 751, 737. HRMS (ESI⁺): [M+H]⁺ found 363.1275; calculated for $[\text{C}_{20}\text{H}_{19}\text{N}_4\text{OS}]^+$ 363.1280. mp 162–163°C.

1-Methyl-1H-indazole-3-carbaldehyde (14). 1H-Indazole-3-carbaldehyde (**11**) (730 mg, 5 mmol) in dry MeCN (5 mL) was treated with iodomethane (0.50 mL, 1.5 eq.) in presence of K_2CO_3 (1.0 g, 1.5 eq.). The solution was refluxed for 16 h, and then after cooling down to room temperature, extracted 3 times with EtOAc. The crude mixture was composed of N₁ and N₂ methylated products with a ratio of 75:15 respectively (determined by ^1H NMR spectroscopy). Both isomers were isolated by flash chromatography (cyclohexane: DCM: EtOAc 65:30:5) (464 mg, white amorphous solid, 58% yield of isolated product). ^1H NMR (CDCl_3 , 300 MHz). δ (ppm) 10.23 (s, 1H), 8.31 (dt, 1H, *J* 8.0, 1.0 Hz), 7.54 – 7.45 (m, 2H), 7.37 (ddd, 1H, *J* 8.0, 5.5, 2.5 Hz), 4.20 (s, 3H). ^{13}C NMR (CDCl_3 , 75 MHz). δ (ppm) 186.7, 143.1, 141.5, 127.6, 124.2, 122.4, 122.2, 109.5, 36.7. IR. ν (cm^{-1}) 3059, 2949, 2792, 1671, 1474, 1426, 1254, 1060, 788, 749, 741. HRMS (ESI⁺): [M+H]⁺ found 161.0716; calculated for $[\text{C}_9\text{H}_9\text{N}_2\text{O}]^+$ 161.0715. mp 62–63°C.

2-Methyl-2H-indazole-3-carbaldehyde (15). Isolated together with 1-methyl-1H-indazole-3-carbaldehyde (**14**) (104 mg, white solid, 13% yield of isolated product). ^1H NMR (CDCl_3 , 300 MHz). δ (ppm) 10.28 (s, 1H), 8.03 – 7.94 (m, 1H), 7.85 – 7.77 (m, 1H), 7.42 – 7.30 (m, 2H), 4.48 (s, 3H). ^{13}C NMR (CDCl_3 , 75 MHz). δ (ppm) 177.5, 147.6, 130.5, 126.8, 126.4, 125.2, 118.7, 118.3, 40.9. IR. ν (cm^{-1}) 2954, 2833, 1673, 1457, 1431, 1291, 1191, 1048, 780, 743. HRMS (ESI⁺): [M+H]⁺ found 161.0713; calculated for $[\text{C}_9\text{H}_9\text{N}_2\text{O}]^+$ 161.0715. mp 65–66°C.

Acknowledgements

This work has been supported by ANR Phinact (ANR-19-CE18-0006). This work has also been partially supported by University of Rouen Normandy, the Centre National de la Recherche Scientifique (CNRS), INSA Rouen Normandy, European Regional Development Fund (ERDF), Labex SynOrg (ANR-11-LABX-0029), Carnot Institute I2C, and the graduate school for research XL-Chem (ANR-18-EURE-0020XL CHEM). Mass spectrometry, IR and melting pot measurements were carried by Albert Marcual (CNRS) and Patricia Martel (Université de Rouen).

Supplementary Material

^1H NMR, NOESY and ^{13}C NMR spectra associated with compounds reported in this article are available as supplementary information.

References

1. Thangadurai, A.; Minu, M.; Wakode, S.; Agrawal, S.; Narasimhan, B. *Med Chem Res* **2012**, *21*, 1509–1523. <https://doi.org/10.1007/s00044-011-9631-3>
2. Tandon, N.; Luxami, V.; Kant, D.; Tandon, R.; Paul, K. *RSC Adv.* **2021**, *11*, 25228–25257. <https://doi.org/10.1039/D1RA03979B>

3. Mal, S.; Malik, U.; Mahapatra, M.; Mishra, A.; Pal, D.; Paidesetty, S. K. *Drug Dev. Res.* **2022**, *83*, 1469–1504.
<https://doi.org/10.1002/ddr.21979>
4. Lian, Y.; Bergman, R. G.; Lavis, L. D.; Ellman, J. A. *J. Am. Chem. Soc.* **2013**, *135*, 7122–7125.
<https://doi.org/10.1021/ja402761p>
5. Cheng, Y.; Li, G.; Liu, Y.; Shi, Y.; Gao, G.; Wu, D.; Lan, J.; You, J. *J. Am. Chem. Soc.* **2016**, *138*, 4730–4738.
<https://doi.org/10.1021/jacs.5b09241>
6. Starck, M.; Kadjane, P.; Bois, E.; Darbouret, B.; Incamps, A.; Ziesel, R.; Charbonnière, L. *J. Chem. Eur. J.* **2011**, *17*, 9164–9179.
<https://doi.org/10.1002/chem.201100390>
7. El-Sayed, M. A. *J. Chem. Phys.* **2004**, *38*, 2834–2838.
<https://doi.org/10.1063/1.1733610>
8. Boujut, M.; Chevalier, A.; Schapman, D.; Bénard, M.; Galas, L.; Gallavardin, T.; Franck, X. *Dyes Pig.* **2022**, *198*, 109988.
<https://doi.org/10.1016/j.dyepig.2021.109988>
9. Catalan, J.; del Valle, J. C.; Claramunt, R. M.; Boyer, G.; Laynez, J.; Gomez, J.; Jimenez, P.; Tomas, F.; Elguero, J. *J. Phys. Chem.* **1994**, *98* (41), 10606–10612.
<https://doi.org/10.1021/j100092a035>
10. Catalan, *Arkivoc* **2013**, (2), 57–70.
<https://doi.org/10.3998/ark.5550190.p008.082>
11. Ghanem, T.; Vincendeau, T.; Simón Marqués, P.; Hossein Habibi, A.; Abidi, S.; Yassin, A.; Dabos-Seignon, S.; Roncali, J.; Blanchard, P.; Cabanetos, C. *Mater. Adv.* **2021**, *2*, 7456–7462.
<https://doi.org/10.1039/D1MA00798J>
12. Neto, B. A. D.; Correa, J. R.; Spencer, J. *Chem. Eur. J.* **2022**, *28*, e202103262.
<https://doi.org/10.1002/chem.202103262>
13. Neto, B. A. D.; Lapis, A. A. M.; da Silva Júnior, E. N.; Dupont, J. *Eur. J. Org. Chem.* **2013**, *2013*, 228–255.
<https://doi.org/10.1002/ejoc.201201161>
14. Yang, W.; Yang, Z.; Xu, L.; Zhang, L.; Xu, X.; Miao, M.; Ren, H. *Angew. Chem. Int. Ed.* **2013**, *52*, 14135–14139.
<https://doi.org/10.1002/anie.201306632>
15. Wang, J.; Shi, D.; Wang, Z.; Ren, F.; Li, X.; You, Y.; Liu, X.; Lou, Y. *J. Org. Chem.* **2023**, *88*, 13049–13056.
<https://doi.org/10.1021/acs.joc.3c01211>
16. Teguh, S. C.; Klonis, N.; Duffy, S.; Lucantoni, L.; Avery, V. M.; Hutton, C. A.; Baell, J. B.; Tilley, L. *J. Med. Chem.* **2013**, *56*, 6200–6215.
<https://doi.org/10.1021/jm400656s>

17. Yu, J.; Hong, Z.; Yang, X.; Jiang, Y.; Jiang, Z.; Su, W. *J. Org. Chem.* **2018**, *14*, 786–795.
<https://doi.org/10.3762/bjoc.14.66>
18. Chekal, B. P.; Guinness, S. M.; Lillie, B. M.; McLaughlin, R. W.; Palmer, C. W.; Post, R. J.; Sieser, J. E.; Singer, R. A.; Sluggett, G. W.; Vaidyanathan, R.; Withbroe, G. J. *Org. Process Res. Dev.* **2014**, *18*, 266–274.
<https://doi.org/10.1021/op400088k>
19. Yu, J.; Yang, X.; Wu, C.; Su, W. *J. Org. Chem.* **2020**, *85*, 1009–1021.
<https://doi.org/10.1021/acs.joc.9b02951>
20. Naas, M.; El Kazzouli, S.; Essassi, E. M.; Bousmina, M.; Guillaumet, G. *Org. Lett.* **2015**, *17*, 4320–4323.
<https://doi.org/10.1021/acs.orglett.5b02136>
21. Xiao, H.; Ye, K.; Liu, C.; Yang, X.; Sun, J.; Lu, R. *Dyes Pigm.* **2023**, *215*, 111241.
<https://doi.org/10.1016/j.dyepig.2023.111241>
22. Chevalier, A.; Ouahrouch, A.; Arnaud, A.; Gallavardin, T.; Franck, X. *RSC Adv.* **2018**, *8*, 13121–13128.
<https://doi.org/10.1039/C8RA01546E>
23. Heravi, M. M.; Behbahani, F. K.; Oskooie, H. A.; Hekmat Shoar, R. *Tet. Let.* **2005**, *46* (15), 2543–2545.
<https://doi.org/10.1016/j.tetlet.2005.02.094>
24. Hocek, M.; Dvořáková, H. *J. Org. Chem.* **2003**, *68*, 5773–5776.
<https://doi.org/10.1021/jo034351i>
25. Evertsson, E.; Inghardt, T.; Lindberg, J.; Linusson, A.; Giordanetto, F. *Therapeutic Agents I*. WO2005066132 (A1), July 21, **2005**.
26. Jung Son, H.; He, F.; Carsten, B.; Yu, L. *J. Mater. Chem.* **2011**, *21*, 18934–18945.
<https://doi.org/10.1039/C1JM12388B>
27. Reichardt, C. *Chem. Rev.* **1994**, *94*, 2319–2358.
<https://doi.org/10.1021/cr00032a005>
28. Rurack, K.; Spieles, M. *Anal. Chem.* **2011**, *83*, 1232–1242.
<https://doi.org/10.1021/ac101329h>

This paper is an open access article distributed under the terms of the Creative Commons Attribution (CC BY) license (<http://creativecommons.org/licenses/by/4.0/>)